J|A|C|S ARTICLES

Published on Web 10/28/2009

Synthesis of PbS Nanorods and Other Ionic Nanocrystals of Complex Morphology by Sequential Cation Exchange Reactions

Joseph M. Luther, Haimei Zheng, Bryce Sadtler, and A. Paul Alivisatos*

Materials Science Division, Lawrence Berkeley National Laboratory, Berkeley, California 94705, and Department of Chemistry, University of California, Berkeley, California 94720-1460

Received August 2, 2009; E-mail: alivis@berkeley.edu

Abstract: We show that nanocrystals (NCs) with well-established synthetic protocols for high shape and size monodispersity can be used as templates to independently control the NC composition through successive cation exchange reactions. Chemical transformations like cation exchange reactions overcome a limitation in traditional colloidal synthesis, where the NC shape often reflects the inherent symmetry of the underlying lattice. Specifically we show that full or partial interconversion between wurtzite CdS, chalcocite Cu_2S, and rock salt PbS NCs can occur while preserving anisotropic shapes unique to the as-synthesized materials. The exchange reactions are driven by disparate solubilites between the two cations by using ligands that preferentially coordinate to either monovalent or divalent transition metals. Starting with CdS, highly anisotropic PbS nanorods are created, which serve as an important material for studying strong two-dimensional quantum confinement, as well as for optoelectronic applications. In NC heterostructures containing segments of different materials, the exchange reaction can be made highly selective for just one of the components of the heterostructure. Thus, through precise control over ion insertion and removal, we can obtain interesting CdS|PbS heterostructure nanorods, where the spatial arrangement of materials is controlled through an intermediate exchange reaction.

Introduction

Rational design of nanoparticles has led to material systems with fascinating properties.[1−5] Size- and shape-controlled nanocrystal growth is intensely researched for electro-optical, catalytic, and medical device applications. The combination of composition and morphology programs specific functionality in nanocrystals (NCs) for incorporation into novel device architectures. For example, anisotropic nanorods and nanotetrapods are used in photovoltaic devices, where two-dimensional quantum confinement controls the semiconductor bandgap and the elongated third dimension improves electron transport compared to that found for spherical NCs in bulk heterojunction devices.[6] CdSe nanorods show shape-dependent polarized photoluminescence.[7] Noble metal particles with shape control give rise to differing plasmonic activity, thus allowing for multicolor cellular labeling.[8,9] Metal nanoparticle shapes with more edge atoms also show enhanced catalytic properties. Fundamental studies of electrical transport in a single NC become feasible through the controlled growth of 1D nanostructures, where different sites along the nanostructure can be independently contacted.[10−12] Therefore, in addition to size and composition, the shape control of NCs demonstrates an important variable to adapt the properties for various applications.

Solution-phase synthetic methods for colloidal NCs are intensely studied as we envision and design specific shapes for combinations of properties.[13−16] However, in traditional nucleation and growth, their resulting size, shape, and composition are often interdependent. Methods for independently tuning one parameter (e.g., composition) while preserving the other two (e.g., size and shape) would enable more systematic control over the resulting NC properties. We and others have demonstrated that ionic NCs can be used as starting materials where the composition is altered post synthesis by exchanging either the

(1) Jun, Y. W.; Choi, J. S.; Cheon, J. *Angew. Chem., Int. Ed.* **2006**, *45*, 3414–3439.
(2) Burda, C.; Chen, X.; Narayanan, R.; El-Sayed, M. A. *Chem. Rev.* **2005**, *105*, 1025–1102.
(3) Alivisatos, A. P. *Science* **1996**, *271*, 933–937.
(4) Kanaras, A. G.; Sonnichsen, C.; Liu, H. T.; Alivisatos, A. P. *Nano Lett.* **2005**, *5*, 2164–2167.
(5) Manna, L.; Milliron, D. J.; Meisel, A.; Scher, E. C.; Alivisatos, A. P. *Nat. Mater.* **2003**, *2*, 382–385.
(6) Huynh, W. U.; Dittmer, J. J.; Alivisatos, A. P. *Science* **2002**, *295*, 2425–2427.
(7) Hu, J. T.; Li, L. S.; Yang, W. D.; Manna, L.; Wang, L. W.; Alivisatos, A. P. *Science* **2001**, *292*, 2060–2063.
(8) Jin, R. C.; Cao, Y. W.; Mirkin, C. A.; Kelly, K. L.; Schatz, G. C.; Zheng, J. G. *Science* **2001**, *294*, 1901–1903.
(9) Link, S.; El-Sayed, M. A. *J. Phys. Chem. B* **1999**, *103*, 8410–8426.
(10) Cui, Y.; Banin, U.; Bjork, M. T.; Alivisatos, A. P. *Nano Lett.* **2005**, *5*, 1519–1523.
(11) Tian, B. Z.; Zheng, X. L.; Kempa, T. J.; Fang, Y.; Yu, N. F.; Yu, G. H.; Huang, J. L.; Lieber, C. M. *Nature* **2007**, *449*, 885-U8.
(12) Trudeau, P. E.; Sheldon, M.; Altoe, V.; Alivisatos, A. P. *Nano Lett.* **2008**, *8*, 1936–1939.
(13) He, J.; Lo, S. S.; Kim, J. H.; Scholes, G. D. *Nano Lett.* **2008**, *8*, 4007–4013.
(14) Kudera, S.; Carbone, L.; Casula, M. F.; Cingolani, R.; Falqui, A.; Snoeck, E.; Parak, W. J.; Manna, L. *Nano Lett.* **2005**, *5*, 445–449.
(15) Mokari, T.; Sztrum, C. G.; Salant, A.; Rabani, E.; Banin, U. *Nat. Mater.* **2005**, *4*, 855–863.
(16) Smith, A. M.; Mohs, A. M.; Nie, S. *Nat. Nanotechnol.* **2009**, *4*, 56–63.

cation or anion with a substitutional ion from solution.[17−19] For example, CdSe NCs can be converted to Ag_2Se with surprising efficiency by simply injecting an alcoholic solution of Ag^+ ions into a suspension of CdSe NCs in toluene.[20] The high surface-to-volume ratio makes the entire NC lattice accessible to solid-state diffusion. Thus, the transformation occurs spontaneously (<1 s) at room temperature and is apparent by a color change (from red to brown) due to different bandgap energies of CdSe and Ag_2Se. Furthermore, the exchange reaction can be reversed to obtain the original bright red solution of CdSe NCs, leading to the near complete recovery of the original exciton spectrum, with only a small change in size-dependent features. By manipulating the ion solubility with coordinating molecules, here we show that the reverse reaction (conversion from the 1+ to 2+ cation) can provide a pathway to new materials.

The thermodynamic driving force for exchange between two cations can be controlled by the solvent and surfactant system based on their relative solvation energies in the prescence of a particular coordinating species.[20,21] In the CdSe−Ag_2Se pair, the forward exchange (from CdSe to Ag_2Se) is thermodynamically driven by the preferential solvation of Cd^{2+} ions relative to Ag^+ in methanol (MeOH). The reverse exchange from Ag_2Se to CdSe is favored by the addition of Cd^{2+}, along with tributylphosphine (TBP). These exchange reactions can be qualitatively understood in terms of hard−soft acid−base theory, where the monovalent Ag^+ cation is softer than the divalent Cd^{2+} cation.[22] Thus, MeOH, a hard base, preferentially binds Cd^{2+} cations, while the soft base, TBP, binds strongly to Ag^+ cations. Several other examples of Cd^{2+} exchange in CdS(Se,Te) NCs with comparatively soft metal ions (Cu^+, Pd^{2+}, Pt^{2+}, Hg^{2+})[18,21,23] using MeOH or water as the solvent and the replacement of soft Ag^+ in Ag_2S NCs with harder metal ions (Pb^{2+}, Zn^{2+}) using TBP have demonstrated the generality of this method.[24] While we were not able to find conditions to directly convert CdS to PbS (due to the similarity of the two ions in their valency, hardness, and electronegativity),[25] through the intermediate conversion of CdS to Cu_2S or Ag_2S, we manipulate the system to produce PbS which retains the original anisotropic nanorod shape.

We employed exchange reactions to sequentially convert CdS NCs first to Cu_2S and then to PbS following the reactions in Scheme 1. Analogous to the examples of cation exchange reactions described above, the exchange of Cu^+ with CdS is promoted with MeOH. After isolation of the NC product, the exchange of Pb^{2+} with Cu_2S NCs is then performed by adding Pb^{2+} and TBP.

During the diffusion and exchange of cations, the anion sublattice is relatively stable, leading to two important consequences. (1) The shapes of anisotropic NCs are generally preserved upon cation exchange, as long as the minimum dimensions of the NC are greater than the reaction zone of the exchange process.[20] (2) A topotaxial relationship exists between the initial and final materials.[18,20] Thus, if the exchange reaction is limited to only part of the NC, a heterostructure is produced where the different compositions share a continuous anion framework.

Scheme 1. Reaction Used To Convert CdS to PbS [a]

$$CdS_{toluene} + 2Cu^+(MeOH) + 2PF_6^-(MeOH) \rightarrow Cu_2S_{toluene} + Cd^{2+}(MeOH) + 2PF_6^-(MeOH) \quad (1)$$

$$Cu_2S_{toluene} + Pb^{2+}(MeOH) + 2OAc^-(MeOH) + 2TBP_{toluene} \rightarrow PbS_{toluene} + 2Cu^+(TBP) + 2OAc^-(MeOH) \quad (2)$$

[a] PF_6^- is the hexafluorophosphate anion of the copper salt, and OAc^- is the acetate anion of the lead salt. Subscripts indicate suspension, whereas the parentheses denote solvation.

The synthesis of monodisperse cadmium chalcogenide NCs with controllable lengths and diameters has been extensively studied over the past decade, making it a well-suited template material for ion exchange conversion.[26−29] While some shape control of lead chalcogenide NCs has also been demonstrated, they typically have cubic or octahedral symmetry, owing to their cubic crystal structure.[30] Elongated structures have been synthesized through oriented attachment of PbSe particles into linear chains, but this approach allows for little length control.[31] The full sequential cation exchange process shown here leads to superior monodispersity of the PbS nanorods. Complete sequential cation exchange also allows the optical properties of one NC material to be directly compared to those of another with the same size and shape.

Furthermore, we demonstrate that through the intermediate conversion of CdS to Cu_2S, the fraction of the ends of rod-shaped NCs converted to PbS can also be controlled. Alternatively, partial Ag^+ exchange can serve as the intermediate step, which produces a striped or superlattice heterostructure morphology.[17] Thus, the spatial arrangement of the components of the heterostructure (i.e., end-on conversion of the nanorod versus striped structure) is controlled via the first exchange reaction, and the final composition is determined by the second.

Experimental Section

Spherical Cu_2S Nanocrystals. A slightly modified version of the procedure described by Wu et al.[32] is followed to synthesize Cu_2S: 104 mg of ammonium diethyldithiocarbamate (Aldrich), 10 mL of 1-dodecanethiol (≥98%, Aldrich), and 14 mL of oleic acid (technical grade, 90%, Aldrich) are combined in a 50 mL flask and heated to 180 °C under an argon flow. In a separate flask, 610 mg of copper(II) acetylacetonate (≥99.99% trace metals basis,

(17) Robinson, R. D.; Sadtler, B.; Demchenko, D. O.; Erdonmez, C. K.; Wang, L. W.; Alivisatos, A. P. *Science* **2007**, *317*, 355–358.
(18) Sadtler, B.; Demchenko, D. O.; Zheng, H.; Hughes, S. M.; Merkle, M. G.; Dahmen, U.; Wang, L. W.; Alivisatos, A. P. *J. Am. Chem. Soc.* **2009**, *131*, 5285–5293.
(19) Dloczik, L.; Konenkamp, R. *Nano Lett.* **2003**, *3*, 651–653.
(20) Son, D. H.; Hughes, S. M.; Yin, Y. D.; Alivisatos, A. P. *Science* **2004**, *306*, 1009–1012.
(21) Wark, S. E.; Hsia, C. H.; Son, D. H. *J. Am. Chem. Soc.* **2008**, *130*, 9550–9555.
(22) Martell, A. E.; Hancock, R. D. *Metal Complexes in Aqueous Solutions*; Plenum Press: New York, 1996.
(23) Mews, A.; Eychmuller, A.; Giersig, M.; Schooss, D.; Weller, H. *J. Phys. Chem.* **1994**, *98*, 934–941.
(24) Camargo, P. H. C.; Lee, Y. H.; Jeong, U.; Zou, Z. Q.; Xia, Y. N. *Langmuir* **2007**, *23*, 2985–2992.
(25) Pearson, R. G. *Inorg. Chem.* **1988**, *27*, 734–740.
(26) Jun, Y. W.; Lee, S. M.; Kang, N. J.; Cheon, J. *J. Am. Chem. Soc.* **2001**, *123*, 5150–5151.
(27) Li, L. S.; Hu, J. T.; Yang, W. D.; Alivisatos, A. P. *Nano Lett.* **2001**, *1*, 349–351.
(28) Manna, L.; Scher, E. C.; Alivisatos, A. P. *J. Am. Chem. Soc.* **2000**, *122*, 12700–12706.
(29) Peng, X. G.; Manna, L.; Yang, W. D.; Wickham, J.; Scher, E.; Kadavanich, A.; Alivisatos, A. P. *Nature* **2000**, *404*, 59–61.
(30) Lee, S. M.; Jun, Y. W.; Cho, S. N.; Cheon, J. *J. Am. Chem. Soc.* **2002**, *124*, 11244–11245.
(31) Cho, K. S.; Talapin, D. V.; Gaschler, W.; Murray, C. B. *J. Am. Chem. Soc.* **2005**, *127*, 7140–7147.
(32) Wu, Y.; Wadia, C.; Ma, W. L.; Sadtler, B.; Alivisatos, A. P. *Nano Lett.* **2008**, *8*, 2551–2555.

Aldrich) and 7 mL of oleic acid are heated under argon to 110 °C. As soon as the solutions are homogeneous and the temperatures are stable, 6 mL of the Cu solution is removed *via* syringe and injected into the other flask. The solution is allowed to react at 180 °C for 6 min, and then the heat is removed. Upon cooling, the black solution is transferred air-free into a vial and centrifuged at 4000 rpm for 5 min. The supernatant is discarded, and the precipitated product is redispersed in hexane and extracted by adding methanol and centrifuging. The final product after several cleaning cycles is roughly 75 mg and suspended in 10 mL of toluene. For reference, the absorbance of the concentration used in the subsequent reaction is shown in the Supporting Information, Figure S1a.

CdS Nanorods. We synthesized CdS nanorods following reports by Robinson and Sadtler et al.[17,18] In brief, 210 mg of CdO (≥99.99% trace metals basis, Aldrich), 2.75 g of tri-*n*-octylphosphine oxide (99%, Acros), and 1.06 g of *n*-octadecylphosphonic acid (PolyCarbon Industries) are heated in a 25 mL flask to 120 °C under vacuum for 30 min. Under argon flow, the solution is heated to 320 °C for 20 min, cooled again to 125 °C, and held under vacuum for 30 min. A stock solution of equimolar tri-*n*-octylphosphine (97%, Strem) and sulfur (flakes, ≥99.99% trace metals basis, Aldrich) (TOP|S) is previously prepared and allowed to stir for 1 day in a glovebox. The temperature of the Cd-phosphonate complex is raised to 320 °C, and 1.5 g of TOP and 1.5 g of TOP|S are added via syringe and allowed to react for 45 min at 315 °C. The solution is then cooled to room temperature, 10 mL toluene is added, and the solution is placed in a centrifuge at 4000 rpm for 10 min. The supernatant is separated, and the product is redispersed in 5−7 mL of toluene and 2 mL of nonanoic acid (purum, ≥97.0% (GC), Fluka). Hexane is added (∼15 mL) slowly until the solution is clear, and then 15 mL of methanol is added, and the solution is centrifuged at 4000 rpm for 10 min. The last step is repeated twice, and a stock solution of the CdS rods is made by dispersing the resulting product in toluene. For reference, the absorbance of the concentration used in the subsequent cation exchange reaction is shown in the Supporting Information, Figure S1b.

Cation Exchange Reactions. Cu_2S spheres are converted to PbS and CdS by room-temperature addition of new cations, similar to the reverse exchange used by Son et al.[20] to convert Ag_2Se back to CdSe. An ion exchange stock solution is prepared to make the conversion more straightforward. First, a 0.15 mM solution of cations is prepared by addition of lead(II) acetate trihydrate (99.999% trace metals basis, Aldrich) for PbS, or cadmium nitrate tetrahydrate (purum p.a., ≥99.0%, Fisher) for CdS, to methanol. Once dissolved, an equal amount of a 0.26 mM solution of tri-*n*-butylphosphine (TBP, 99%, Strem) in toluene is added. TBP is used to promote the exchange in Cu_2S NCs by binding strongly to Cu^+ ions, thus creating a driving force to convert the crystal into PbS or CdS. Control experiments without the use of TBP show extremely slow kinetics or no ion exchange. To perform the exchange, 1 mL of toluene is added to 0.1 mL of the stock solution of Cu_2S NCs in a vial on a stirring plate (with magnetic stir bar) in a glovebox. One milliliter of the ion exchange solution is added. To aid in the solubility of the final product, we also add 10−30 μL of lead oleate or cadmium oleate. Oleate solutions are prepared by following the method described by Pietryga[33] and are stored in a vial in a glovebox on a hot plate at 80 °C. Two milliliters of methanol is added before centrifuging at 3000 rpm to separate the NCs from the solvent and ions. The final product is soluble in nonpolar organic solvents.

Partial and full exchange of CdS nanorods to Cu_2S is well described in a previous report by Sadtler et al.[18] In this case, a solution of tetrakis(acetonitrile)copper(I) hexafluorophosphate (Aldrich) is made in methanol, 0.5 mL is added to 0.5 mL of toluene, and under rapid stirring, 100 μL of the CdS stock solution is added. The color instantly changes to orange-brown, the vial is then centrifuged at 3000 rpm, and the product is suspended in 1 mL of toluene. The concentration of the methanolic solution determines the fraction of the sample converted to Cu_2S. In this case we found that 0.5 mL of a 2 mg/mL Cu solution completely converts the rods to Cu_2S by XRD and UV−vis characterization. Partial exchange was performed by varying the amount of Cu^+ in the solution relative to the 2 mg/mL mark. For full exchange, 10 mg/mL was used to ensure that the entire sample was converted to Cu_2S.

The conversion of the Cu_2S or Ag_2S portions of nanorods to PbS is accomplished in a way similar to the conversion of Cu_2S spheres to PbS. The Cu_2S rods in 1 mL of toluene were converted to PbS rods by using the same cation stock solutions as in the case of the spheres. Only 1 mL of methanol is added before centrifugation to separate the nanorods.

Interfacial Model. The electron diffraction patterns and interface structure were simulated using commercially available software, Crystalkit (http://www.totalresolution.com).

Instrumentation. Absorbance measurements are performed with the NCs suspended in tetrachloroethylene (ACS reagent, ≥99.0%, Sigma-Aldrich) on a Shimadzu 3600 UV−vis−NIR spectrophotometer. Low-magnification TEM images were acquired with a 200 kV LaB6 FEI Tecnai G2 20 high-resolution transmission electron microscope, equipped with a Super TWIN lens. Size histograms and fast Fourier transform (FFT) algorithms were performed using free software, ImageJ (http://rsbweb.nih.gov/ij/index.html). For high resolution, a 200 kV FEI monochromated F20 UT Tecnai transmission electron microscope equipped with a field emission gun, a high-angle annular dark-field detector (HAADF), and a Gatan image filter (GIF) was also used for the TEM characterization. Powder XRD characterization was carried out on a GADDS Hi-Star D8 diffractometer (Bruker) using Co Kα radiation (1.790 Å) and a general area detector. Samples were prepared by deposition on a quartz plate with background subtraction. Accumulation time for each sample was 20 min (10 min/frame). Experimental XRD patterns were compared with those published in the Joint Committee of Powder Diffraction Standards (JCPDS) PDF database for bulk materials (CdS, no. 41-1049; PbS, no. 05-0592; Cu_2S, nos. 26-1116 and 33-0490).

Results

We first discuss a control experiment to properly characterize that the NC size is preserved in the reverse reactions from Cu_2S to PbS or CdS. We synthesized spherical Cu_2S NCs with the high chalcocite phase following the method of Wu et al.[32] Monodisperse Cu_2S NCs with diameters <5 nm are then suspended in toluene for the cation exchange reactions. Transmission electron microscopy (TEM) is used to determine the NC size because of a relative lack of optical absorbance features, a complex X-ray diffraction (XRD) spectrum with no well-resolved peak to measure, and relatively few publications on size/shape control of Cu_2S. Following a method similar to that described for Ag_2Se to CdSe exchange described above, Cu_2S NCs are then transformed to PbS or CdS, where the size-dependent optical properties can be compared.

To convert Cu_2S to PbS or CdS, a solution of Pb^{2+} or Cd^{2+} ions with TBP was prepared, added to Cu_2S NCs in toluene, and allowed to stir for ∼2 h while the color changed from orange-brown to either dark brown for PbS or bright yellow for CdS. The NCs were then separated from the free-floating ions by centrifugation (see Experimental Section). Figure 1 shows TEM images along with XRD and UV−vis absorbance spectra for NCs in all three sulfide compositions (CdS, Cu_2S, and PbS). The TEMs show well-packed, monodisperse particles with similar diameter, aside from small deviations for differing

(33) Pietryga, J. M.; Werder, D. J.; Williams, D. J.; Casson, J. L.; Schaller, R. D.; Klimov, V. I.; Hollingsworth, J. A. *J. Am. Chem. Soc.* **2008**, *130*, 4879–4885.

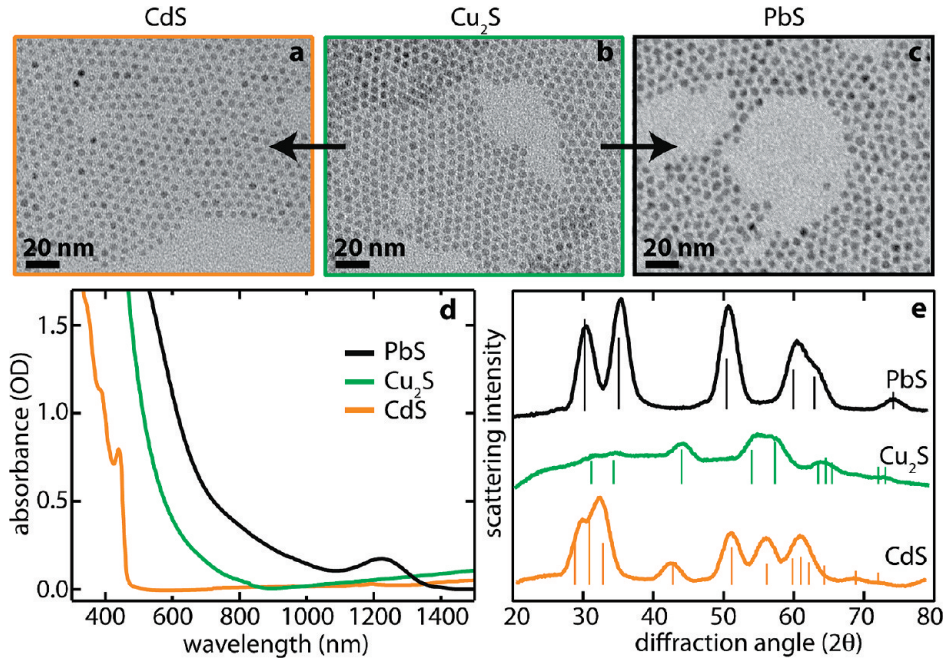

Figure 1. Properties of Cu_2S spherical particles converted to CdS and PbS. (a−c) TEM images of well-packed CdS, Cu_2S, and PbS NCs, respectively. Images are at the same magnification with a scale bar of 20 nm in each image. (d) Identical concentration absorption spectra for NCs of CdS, Cu_2S, and PbS from the same starting material in tetrachloroethylene. The characteristic first exciton peak for CdS (PbS) is at 440 nm (1240 nm), corresponding to a NC diameter of ∼4.8 nm. (e) XRD for an ensemble of NCs of Cu_2S (green). Also shown are traces for the resulting CdS (orange) and PbS (black) from cation exchange of Cu_2S. The JCPDS card file for each material is shown below the spectrum for identification.

lattice constants of the three crystals. Perhaps a better indication of the NC size is inferred from the linear absorption data correlated to published size-dependent extinction coefficients for the well-studied lead and cadmium chalcogenides. Figure 1d shows the absorbance curves for spherical particles. CdS exhibits several sharp excitonic features indicating the high degree of monodispersity. The first exciton peak occurs at 440 nm (2.81 eV), corresponding to a diameter of 4.85 nm.[34] PbS has small effective masses for electrons and holes, which leads to a dramatic blueshift in the bandgap above the bulk value of 0.41 eV when confined below 20 nm, and displays a wealth of fascinating properties at the nanoscale.[35−38] In the case of our spherical PbS particles created by cation exchange from Cu_2S, the first exciton peak occurs at 1240 nm (1 eV) and corresponds to NCs with diameter of 4.8 nm.[39,40] XRD patterns of the three samples show the initial Cu_2S in the high-temperature chalcocite phase, while the CdS and PbS NCs are in the wurtzite and rock salt phases, respectively. The particle sizes are also verified by applying a Debye−Sherrer fit to the XRD data in Figure 1e.[41]

After verifying that Cu_2S can readily be converted to PbS, we then synthesized rod-shaped CdS NCs using surfactants that promote anisotropic growth of the (001) and (00$\bar{1}$) facets, which become the ends of the nanorods.[28] Recently we have shown that Cu^+ ions will readily exchange with Cd^{2+} by selectively targeting the nanorods' more reactive end facets. We exchanged CdS nanorods to Cu_2S nanorods using this same procedure.[18] The resulting Cu_2S NCs are isolated and then exchanged to PbS just as described above for spherical Cu_2S to PbS conversion. Figure 2a−c shows TEMs of the nanorods throughout the sequential cation exchange. The absorbance spectra for solutions of the nanorods are shown in Figure 2d. The exciton features in the CdS spectrum result from the highly monodisperse nanorod diameter throughout the sample. Since the diameter is much smaller than the length, quantum confinement effects are dominated by this dimension.[5,27] Upon conversion to Cu_2S, a weak exciton peak arises at 850 nm. After the sequential cation exchange to PbS, a well-resolved peak appears at 1440 nm. While several reports exist for rod-shaped PbS crystals,[42−46] no reports to date show featured quantum confined absorption spectra in any of the lead chalcogenides for such anisotropic shapes. This is presumably due to the difficulty of growing highly symmetric rock salt crystals into monodisperse nanorods. Here we take advantage of the abundance of pre-existing work on shape control in cadmium chalcogenides to control the final size and shape of lead chalcogenide crystals with sequential chemical transformations.

The first exciton peak at 1440 nm (0.86 eV) corresponds to spheres with a diameter of 5.7 nm,[39] yet the nanorods produced have a diameter of ∼5 nm, with an average length of ∼26 nm

(34) Yu, W. W.; Qu, L. H.; Guo, W. Z.; Peng, X. G. *Chem. Mater.* **2003**, *15*, 2854–2860.
(35) Ellingson, R. J.; Beard, M. C.; Johnson, J. C.; Yu, P. R.; Micic, O. I.; Nozik, A. J.; Shabaev, A.; Efros, A. L. *Nano Lett.* **2005**, *5*, 865–871.
(36) Ma, W.; Luther, J. M.; Zheng, H. M.; Wu, Y.; Alivisatos, A. P. *Nano Lett.* **2009**, *9*, 1699–1703.
(37) McDonald, S. A.; Konstantatos, G.; Zhang, S. G.; Cyr, P. W.; Klem, E. J. D.; Levina, L.; Sargent, E. H. *Nat. Mater.* **2005**, *4*, 138–142.
(38) Wise, F. W. *Acc. Chem. Res.* **2000**, *33*, 773–780.
(39) Cademartiri, L.; Montanari, E.; Calestani, G.; Migliori, A.; Guagliardi, A.; Ozin, G. A. *J. Am. Chem. Soc.* **2006**, *128*, 10337–10346.
(40) Hyun, B. R.; Zhong, Y. W.; Bartnik, A. C.; Sun, L. F.; Abruna, H. D.; Wise, F. W.; Goodreau, J. D.; Matthews, J. R.; Leslie, T. M.; Borrelli, N. F. *ACS Nano* **2008**, *2*, 2206–2212.
(41) The TEM images in Figure 1a−c are somewhat deceiving because the different cations create stronger contrast for Pb compared to Cd, thus making the PbS NCs appear larger than those of Cu_2S or CdS.
(42) Chen, M.; Xie, Y.; Yao, Z. Y.; Qian, Y. T.; Zhou, G. E. *Mater. Res. Bull.* **2002**, *37*, 247–253.
(43) Li, C.; Shi, G.; Xu, H. Y.; Guang, S. Y.; Yin, R. H.; Song, Y. L. *Mater. Lett.* **2007**, *61*, 1809–1811.
(44) Ni, Y. H.; Liu, H. J.; Wang, F.; Liang, Y. Y.; Hong, J. M.; Ma, X.; Xu, Z. *Cryst. Growth Des.* **2004**, *4*, 759–764.
(45) Wang, S. H.; Yang, S. H. *Langmuir* **2000**, *16*, 389–397.
(46) Warner, J. H.; Cao, H. Q. *Nanotechnology* **2008**, *19*, 305605.

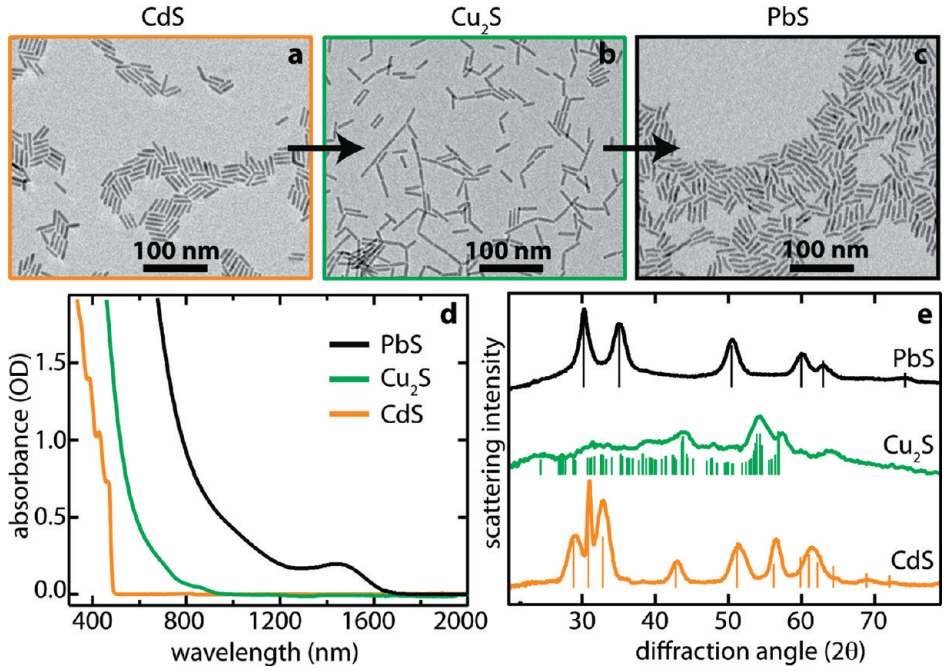

Figure 2. Properties of nanorods of CdS transformed into Cu_2S and then PbS. TEM images of as-synthesized CdS (a), intermediate Cu_2S (b), and the final PbS (c) nanorods. The scale bars are 100 nm long, and the arrows indicate the order of cation exchange products. See Supporting Information, Figure S2, for size histograms of the nanorod images. (d) Absorption spectra for CdS (orange), Cu_2S (green), and PbS (black) nanorods with identical concentration. (e) XRD patterns for the different materials. The lines under the spectra are the JCPDS patterns for each material. Here, we assign the Cu_2S nanorods to the low chalcocite phase.[18]

(see Supporting Information, Figure S2, for length histograms of the nanorods). Figure 2e shows the XRD patterns for each of the nanorod samples, along with the JCPDS card files to identify each material. The XRD provides the best evidence that the final nanorods are in the PbS rock salt phase, which is supported by a typical PbS absorption spectrum shown in Figure 2d. Furthermore, just as in the case of cadmium chalcogenides, the bandgap can be tuned by varying the diameter of the nanorod.[27] In the Supporting Information (Figure S3), additional absorption spectra show that the bandgap can be increased to greater than 1 eV (i.e., increased confinement) with decreasing diameter, independent of the nanorod length.

The degree of cation exchange in nanorods from CdS to Cu_2S can be controlled by the amount of Cu^+ ions added to the solution.[18] For example, if the ratio of Cu^+:Cd^{2+} is restricted to 1, then, on average, the nanorods are composed of 50% CdS and 50% Cu_2S (because two Cu^+ cations are needed to replace each Cd^{2+} cation for charge balance). Here, we followed this procedure to create a series of heterostructured nanorods from the same CdS sample as in Figure 2a to have varying amounts of Cu_2S within each nanorod. Each was then exposed to an excess of Pb^{2+} ions (the same amount as used for the full exchange in Figure 2). We find that the final nanoheterostructures are composed only of CdS and PbS, where only the Cu_2S segments have been converted to PbS. Figure 3 shows basic characterization of CdS|PbS nanorod heterostructures as a function of the amount of Cu^+ ions that were added to the CdS solution. While previous work has shown the conversion of lead chalcogenides directly to cadmium chalcogenides (the reverse transformation of our work, limited to partial conversion in spheres to form core−shells), these reactions were explained by stronger bonding of the Cd-chalcogenide lattice, rather than the relative solubility of the ions.[33,47] Our experiment demonstrates that the reaction CdS + Pb^{2+} → PbS + Cd^{2+} is far less favorable under our conditions than Cu_2S + Pb^{2+} → PbS + $2Cu^+$ (see Scheme 1). Presumably, the soft base, TBP, binds more strongly to the monovalent Cu^+ cation compared to Cd^{2+} or Pb^{2+}, providing substantially more control.

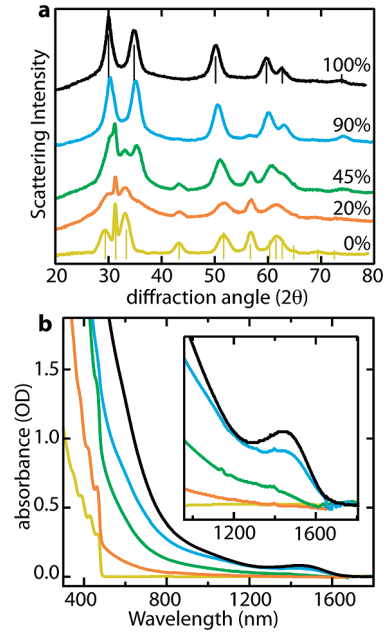

Figure 3. (a) XRD spectra for nanorods of CdS that have been partially converted to Cu_2S before being exposed to Pb^{2+} ions. The nanorods are a mixture of wurtzite CdS and rock salt PbS. The JCPDS card files for CdS (yellow) and PbS (black) are shown under the respective spectra. (b) Absorption spectra of heterostructured CdS|PbS nanorods. Nanorods partially exchanged to Cu_2S and then to PbS show absorbance features which are a superposition of those for PbS and CdS. However, the intensity and peak position of the PbS first exciton peak are dependent on the amount of Cu^+ ions added during the intermediate step.

In Figure 3a, the XRD patterns of the product NCs only show contributions from CdS and PbS and are clearly a convolution of the two diffraction patterns, where the relative fraction of each is controlled by the amount of Cu^+ ions added in the intermediate step and is independent of the amount of Pb^{2+} ions added. Upon exposing CdS to an increasing Cu^+:Cd^{2+} ion ratio, the CdS to Cu_2S conversion proceeds further, and the resulting NCs show diffraction patterns with more PbS than CdS, as indicated by the decrease in the peaks at $2\theta = 43°$ and 57° and the appearance of two distinct peaks instead of three near $2\theta = 30°$.

The absorption spectrum of the heterostructured nanorods is shown in Figure 3b. For low conversion ratios, the absorption closely resembles that of CdS, with a characteristic cutoff to the red of 470 nm and a tail extending red, due to the smaller bandgap of PbS. Upon further conversion, the absorbance onset redshifts and develops a well-structured exciton peak at 1440 nm.

A much different morphology of CdS|PbS nanorods is created by using Ag^+ ions to perform the intermediate exchange reaction, rather than Cu^+. In this case, the partial exchange to form CdS|Ag_2S leads to small Ag_2S regions distributed along the sides of the CdS nanorods and, under careful conditions, leads to a superlattice structure in each nanorod with alternating segments of CdS and Ag_2S.[17,48] Thus, the intermediate stage can be used to control the resulting heterostructured topology, as only the Ag^+ ions are replaced by Pb^{2+}, leading to PbS embedded in CdS (see Supporting Information, Figure S4).

Due to the differing crystal structures of wurtzite CdS (hexagonal lattice with four nearest neighbor atoms) and rock salt PbS (cubic lattice with six nearest neighbor atoms), we employed high-resolution TEM (HRTEM) to examine the structure of nanorods fully converted from CdS to PbS (Figure 4) and partially converted nanorods to study the interface between the two crystalline components (Figure 5).

Figure 4 shows a HRTEM image of a 25 × 5 nm PbS nanorod. We observe grain boundaries appearing in the fully exchanged PbS nanorods. However, a fast Fourier transform (FFT) of the single grains (as shown in Figure 4b−d) shows that all regions within the nanorod are PbS of the same rock salt phase with an in-plane rotation between the grains. We note that, since the S sublattice of Cu_2S is very similar to that of CdS, there is little change in the shape of the nanorods during cation exchange between Cu^+ and Cd^{2+}.[18] By studying the heterostructured CdS|PbS rods from partial exchange of CdS to Cu_2S, we can understand the formation of such "multigrain" morphology of PbS nanorods.

Figure 5 shows an HRTEM image of a nanorod having undergone partial exchange to Cu_2S, followed by conversion of the Cu_2S portion to PbS. The Cu_2S is completely removed, and the resulting particle has a rock salt PbS grain attached epitaxially to the wurtzite CdS phase, with $(\bar{1}11)_{PbS}/(00\bar{2})_{CdS}$ and $(\bar{2}\bar{2}4)_{PbS}/(1\bar{1}0)_{CdS}$. The long dimension of the CdS nanorod is the [002] direction, as can be verified by the FFT shown in Figure 5c. Correspondingly, the sharpest peak in the XRD pattern, at $2\theta = 32°$, belongs to the (002) plane in Figure 3a (bottom trace). Upon cation exchange to PbS, we use the FFT of the HRTEM images to confirm that the elongated dimension of CdS transforms to the [111] direction of PbS. The XRD for the completely exchanged PbS rods in Figure 3a shows a sharpened (111) peak at $2\theta = 29°$, due to longer diffraction coherence.

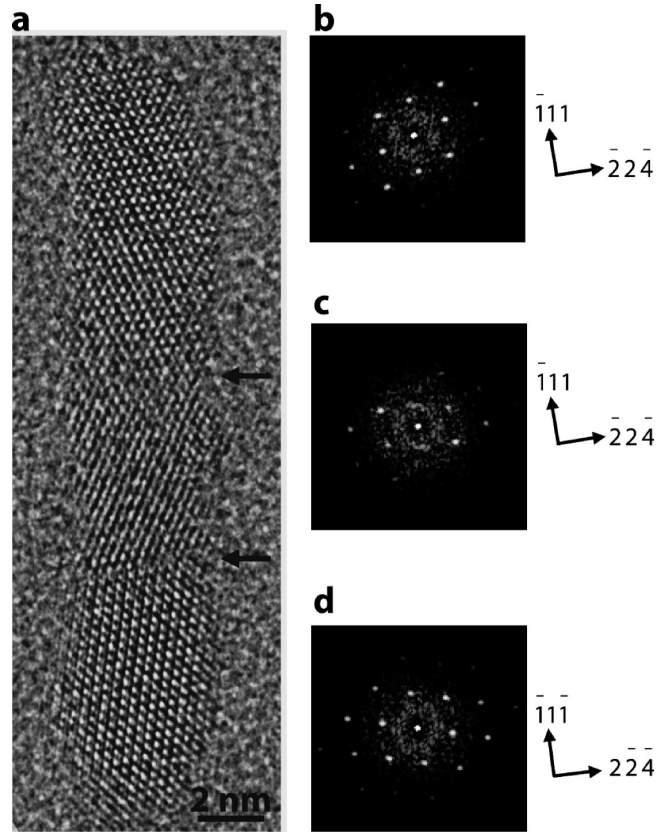

Figure 4. (a) HRTEM image of a fully converted PbS nanorod. Arrows indicate grain boundaries. (b−d) FFT patterns of the top, middle, and bottom sections of the nanorod as separated by the arrows in (a). Each FFT pattern shows a well-defined diffraction pattern corresponding to the [110] zone diffraction of a rock salt PbS crystal.

Epitaxial connections between wurtzite and rock salt phases within NCs have been seen and discussed in the literature.[14,33,47,49] The atomic structure and interface that are built on the basis of such observations (Figure 5f) show lattice distortions of the S framework in addition to the displacement of cations between the two phases. As the Pb^{2+}−Cu^+ exchange front moves along the NCs during the reaction, these displacements induce the misalignment of the long axis of the PbS segment of the nanorod relative to that of the stationary CdS portion (see Figure 5a). Cation exchange may start at one or both ends of the nanorod, leading to different lattice distortions at either end.[18] Therefore, as the reaction fronts meet in the case of complete exchange, a grain boundary can form. As can be seen in the fully converted PbS nanorod in Figure 4, the FFT of panels b and c are the same face and orientation, and panel d shows a different orientation. The grains meet at the lower of the two arrows in panel a. However, in the case of heterostructured particles, each PbS segment within a nanorod is single crystalline (Figure 5a).

Conclusion

We have shown the ability to independently control the shape, topology, and final chemical composition of colloidal nanocrystals in three separate steps. The nucleation and growth of

(47) Lambert, K.; De Geyter, B.; Moreels, I.; Hens, Z. *Chem. Mater.* **2009**, *21*, 778–780.
(48) Demchenko, D. O.; Robinson, R. D.; Sadtler, B.; Erdonmez, C. K.; Alivisatos, A. P.; Wang, L.-W. *ACS Nano* **2008**, *2*, 627–636.
(49) Zhou, H. S.; Honma, I.; Komiyama, H.; Haus, J. W. *J. Phys. Chem.* **1993**, *97*, 895–901.

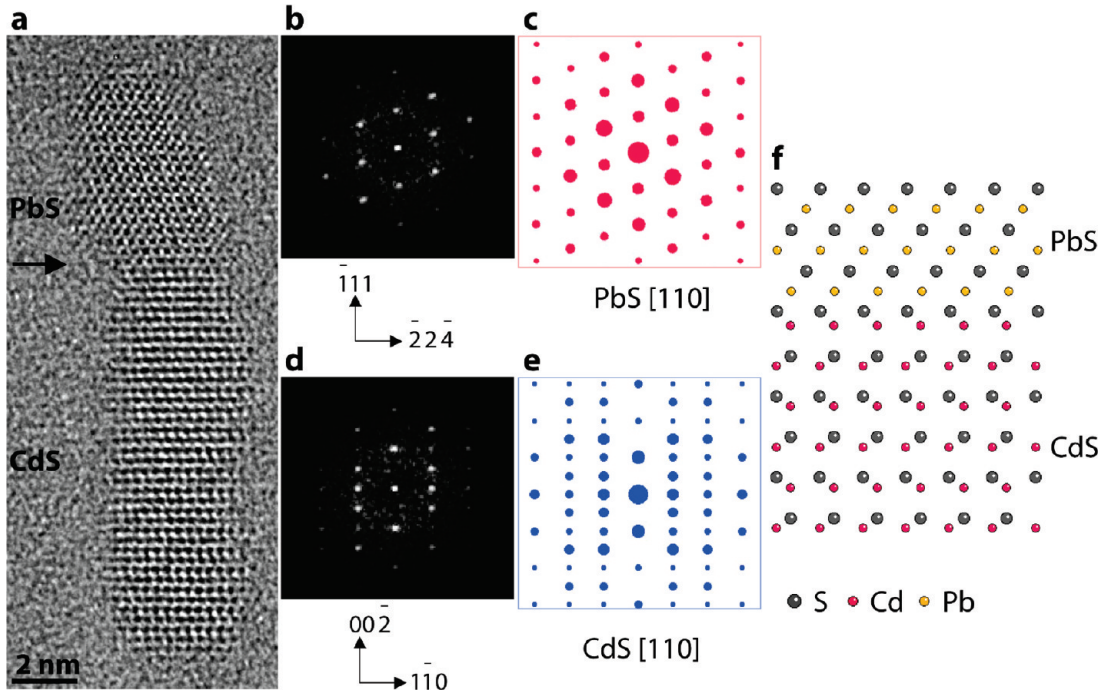

Figure 5. HRTEM image and simulated atomic structure displaying the interface of CdS|PbS nanoheterostructures. (a) HRTEM image showing epitaxy between rock salt PbS and wurtzite CdS. An arrow highlights the interface. (b) FFT pattern of the PbS grain in (a). (c) Simulated diffraction pattern of rock salt PbS [110]. (d) FFT pattern of the CdS grain in (a). (e) Simulated diffraction pattern of wurtzite CdS [110]. (f) Atomic structure and interfacial model between PbS and CdS viewed from [110] of both phases.

the NC starting material determine the shape, while a sacrificial exchange into an intermediary composition allows for conversion to a heterostructure containing two materials with control of their topology. The second exchange reaction then determines the final chemical composition of the crystal. This method has enabled the construction of the first example of highly monodisperse PbS nanorods that will undoubtedly be useful materials for various applications. By precisely controlling ion insertion and removal (through partial Cu^+ or Ag^+ exchange), nanorod heterostructures with different morphologies can be obtained. The selectivity for the second exchange reaction to convert only the Cu_2S (Ag_2S) portion of the heterostructures to PbS is akin to regioselective transformations of functional groups in organic molecules. Such selectivity is essential for the creation of complicated nanostructures over multistep synthesis. The successive cation exchange principle demonstrated here provides a unique route to synthesize epitaxial heterogeneous nanostructures in a variety of material combinations and shapes.

Acknowledgment. This work was supported by the Director, Office of Science, Office of Basic Energy Sciences, Materials Sciences and Engineering Division, of the U.S. Department of Energy under Contract No. DE-AC02-05CH11231. The authors acknowledge the National Center for Electron Microscopy for providing the advanced electron microscopy facilities for this work. J.M.L. thanks Jon Owen for helpful discussion.

Supporting Information Available: Additional absorbance spectra, length histograms, and TEM images. This material is available free of charge via the Internet at http://pubs.acs.org.

JA906503W